

## **In vitro** evaluation of polymeric formulations designed for use in alveolar osteitis

Karolina M. Nowak,<sup>1</sup> Arkadiusz Szterk,<sup>2</sup> Tomasz Szymborski,<sup>3</sup> Karolina Rudnicka,<sup>4</sup> Piotr Fiedor,<sup>5</sup> Kazimiera H. Bodek<sup>1</sup>

<sup>1</sup>Department of Applied Pharmacy, Faculty of Pharmacy, Medical University of Lodz, Muszynskiego 1, 90-151 Lodz, Poland

<sup>2</sup>Department of Food Analysis, Prof. Wacław Dąbrowski Institute of Agricultural and Food Biotechnology, Rakowiecka 36, 02-532 Warsaw, Poland

<sup>3</sup>Department of Soft Condensed Matter, Institute of Physical Chemistry, Polish Academy of Sciences, Kasprzaka 44/52, 01-224 Warsaw, Poland

<sup>4</sup>Department of Immunology and Infectious Biology, Faculty of Biology and Environmental Protection, University of Lodz, Banacha 12/16, 90-237 Lodz, Poland

<sup>5</sup>Department of General and Transplantation Surgery, Transplantation Institute, Warsaw Medical University, Nowogrodzka 59, 02-006 Warsaw, Poland

Correspondence to: K. H. Bodek (E-mail: kazimiera.bodek@umed.lodz.pl)

**ABSTRACT:** In this article, we present a potential use of biodegradable polymers as a drug-delivery system designed for alveolar osteitis (AO) management. The release characteristics of lidocaine hydrochloride from alginate or hyaluronate xerogels, which covered the microcrystalline chitosan scaffold, were examined as drug carriers, wound dressings, and potential devices in bone regeneration. The materials were characterized by Fourier transform infrared spectroscopy to confirm that there was no additional covalent bonding between the polymeric membranes and the anesthetic agent. Surface-eroding matrices (ca. 120  $\mu\text{m}$ ) encapsulated the main substance, and the morphologies of all of the structures were measured by scanning electron microscopy. Positive results were obtained, and the data suggested an important impact of materials selection on the physicochemical properties and drug release. Additionally, the mechanical properties, such as the hardness, adhesiveness, springiness, and cohesiveness, of the tested materials were evaluated. A study of the swelling confirmed one of the assumptions that the materials could be used as a potential wound dressing and emphasized the resistance of the materials in the condition imitating the movement of the masticatory system. A cytotoxicity test of the formulations was performed to prove the materials' nontoxicity. The aim of this study was to design and propose an *in vitro* evaluation of a new drug formulation as a potential application for the treatment of AO. © 2015 Wiley Periodicals, Inc. *J. Appl. Polym. Sci.* **2016**, *133*, 42991.

**KEYWORDS:** biodegradable; biomaterials; crosslinking; drug-delivery systems; swelling

Received 12 February 2015; accepted 27 September 2015

DOI: 10.1002/app.42991

### INTRODUCTION

Recently, there has been an urgent need for new, more advanced controlled drug-delivery systems. Appropriate materials selection, manufacturing process, and laboratory techniques are crucial in the process of drug delivery. Also, a deep understanding of the chemical structure of the materials used is essential for predicting the usefulness of the formulations obtained. However, there are still some medical problems whose treatments are not well established. Such an example is alveolar osteitis (AO), an inflammation process within alveolar bone that occurs as a result of postoperative complication of tooth extraction. Although the pathoetiology of AO is established, there is still no sufficient treatment available.<sup>1,2</sup> This is because of the complex-

ity of its etiology and the variability of inducing factors. The most convincing hypothesis explaining the etiology of AO was proposed by Birn.<sup>3</sup> According to his studies, the development of AO is a result of the increased fibrinolytic activity and the activation of plasminogen to plasmin, which affects the maintenance of the postextraction blood clot. Currently, the efficiency of AO treatment is not yet appropriate to patient needs.

In this research, we tried to solve this problem. The selection of appropriate materials had a major impact on the successful drug-delivery design. Chitosan was used on the grounds of its various distinctive properties,<sup>4-7</sup> such as its biodegradability, biocompatibility, mucoadhesiveness, nonantigenic, and nontoxicity.<sup>8</sup> Chitosan is a biodegradable cationic polysaccharide

composed of  $\beta(1\rightarrow4)$ -linked D-glucosamine (deacetylated unit) and N-acetyl-D-glucosamine (acetylated unit); it is known to accelerate wound healing and bone formation.<sup>9</sup> It also fosters granulation tissue formation with angiogenesis.<sup>10</sup> Because of its porous structure, surface properties, and biodegradability, this material can be used as a scaffold for the tissue regeneration process.<sup>10</sup> Chitosan has been associated with other biopolymers and with synthetic polymer dispersions in the production of wound dressings. Chitosan–calcium phosphate composites were investigated as injectable resorbable scaffolds for bone tissue regeneration.<sup>11</sup>

A valuable physicochemical modification of chitosan that is used among others as an excipient in drug formulations is microcrystalline chitosan (MCCh), which is obtained in the form of a suspension, powder, or granules.<sup>12,13</sup> A polymer with desired chemical properties is prepared by the appropriate aggregation of macromolecules from aqueous solutions of organic acids (via the neutralization, coagulation, and then precipitation of MCCh).<sup>14</sup> MCCh shows a number of valuable features compared with unmodified chitosan: a higher absorptivity, higher crystallinity, chelating capability, and higher bioactivity. MCCh is a safe and effective biopolymer for the achievement of hemostasis at puncture sites.<sup>15</sup> This natural polysaccharide shows unique biostimulating properties, that is, the reconstruction and vascularization of damaged tissues.<sup>16</sup> The most important and the most extraordinary property MCCh is that the films from the aqueous dispersion directly formed. The film obtained in this process shows excellent adhesion to different types of surfaces and water resistance.<sup>17</sup> The properties mentioned previously present several possibilities for pharmaceutical and medical uses of MCCh. MCCh is also characterized by unique miscibilities with several polymers, substances, and solvents. Because of the type of polymer used (MCCh), it was possible to obtain a compact and homogeneous cone shape. According to the Food and Drug Administration, chitosan has the status of generally recognized as safe.<sup>18</sup> However, because the milieu of AO is consistently exposed to inflammatory agents, such as activated immune cells, cytokines, and chemokines, which enhance potentially occurring cell damage, it is especially important to evaluate the cytotoxic properties of each new formulation. In our previous research, we demonstrated that the formulations based on MCCh with addition plasticizer had different physical and mechanical properties.<sup>19</sup>

In this study, the structure of bilayer formulations was evaluated, and we determined the release profile of lidocaine hydrochloride ( $\text{Lid}_{\text{HCl}}$ ) from polymeric systems. The external surface of the dental formulation was composed of sodium alginate (Alg) or sodium hyaluronate (Hial), and it was used to cover the previously obtained MCCh cone-shaped formulations.<sup>19</sup> Alg is well known in food administration, drug formulation (beads, microspheres, and matrix tablets), and bone and soft tissue regeneration.<sup>20–23</sup> Hial, currently a widely used glycosaminoglycan, is important because of its presence in connective tissue and periodontal ligaments and its use in tissue regeneration, including tissue hydration, proteoglycan organization in the extracellular matrix, and tissue repair.<sup>24,25</sup> The physicochemical properties and different forms of hyaluronate have a large applicable potential, especially in tissue regeneration and wound healing.<sup>26,27</sup>

$\text{Lid}_{\text{HCl}}$  was chosen as a modal substance because of its wide spectrum of application in dentistry and maxillofacial surgery.<sup>28–30</sup> This anesthetic agent, in addition to its primary function, is a membrane stabilizer and phospholipase A2 inhibitor.<sup>31</sup>

The AO complication is important not only because of AO's clinical aspects, such as an enormous pain, but also because of the probability of the incomplete reconstruction of the alveolar bone.<sup>32–34</sup> The main aim of this study was to design and propose an *in vitro* evaluation of a new drug formulation designed for the treatment of AO.

## EXPERIMENTAL

### Materials

MCCh as a 3.88 wt % hydrogel (weight-average molecular weight = 340 kDa, degree of deacetylation = 81.0%, and pH 6.8) was supplied by Institute of Biopolymers and Chemical Fibres (Łódź, Poland). Propylene glycol (GP), glycerol (G) (minimum 88%), phosphoric acid, and Alg were supplied by POCh (Gliwice, Poland). Calcium chloride, sodium chloride, disodium hydrogen phosphate, and monopotassium phosphate were supplied by Chempur (Piekary Śląskie, Poland).  $\text{Lid}_{\text{HCl}}$  was supplied by Amara (Kraków, Poland). Hial, a 1% penicillin/streptomycin solution, 2 mM L-glutamine, and 10% fetal bovine serum were supplied by Sigma-Aldrich Co. (St. Louis, MO). Thiazolyl blue tetrazolium bromide [3-(4,5-dimethylthiazol-2-yl)-2,5-diphenyltetrazolium bromide], dimethyl sulfoxide, and phosphate-buffered saline were supplied by R&D System (Minneapolis, MN). Fast drying silver paint was supplied by Ted Pella, Inc. All of the reagents used were analytical grade.

### Preparation of Polymeric Formulations

The preparations were composed of two parts: external membranes covering an internal cone-shaped scaffold, as shown in Table I. The formulations were made from biodegradable polymers under aseptic conditions (in a laminar box). The inner part consisted of MCCh cone-shaped formulations. It was prepared from a radiation-sterilized (25-kGy) MCCh hydrogel (acc. 600 mg) mixed well with a mechanical stirrer with 20  $\mu\text{L}$  of  $\text{CaCl}_2$  (0.5 mol/L) as a crosslinking agent and 50 mg of the plasticizer propylene glycol. The polymer hydrogel was introduced into an Eppendorf tube and put in a special laminar box for water evaporation. Then, the materials were transferred into a special cone-shaped tube and later placed in an incubator for 24 h. All of the samples were stored at 4°C before further analysis. The outer part consisted of a polymeric film coating made from 15% Alg hydrogel or 3% Hial hydrogel with a plasticizer (propylene glycol or glycerol; Table I) and crosslinking agent (20  $\mu\text{L}$  of 25 mmol/L  $\text{CaCl}_2$ ). This part was prepared by the dissolution of  $\text{Lid}_{\text{HCl}}$  in a previously prepared hydrogel. The drug was added with stirring to keep the viscosity of the hydrogel constant and to maintain a uniform distribution of the drug. This material was used to cover the previously obtained MCCh cone-shaped formulations.<sup>19</sup> It was placed on Petri dishes and kept in a desiccator for 7 days. All of the ingredients were sterilized, and the formulations were prepared in a laminar box. The quantities of polymeric materials and excipients (plasticizer and a crosslinking agent) summarized in Table I were selected on the basis of previous studies<sup>19</sup> to produce a system with a

**Table I.** Compositions of the Preparations

Sample number	Internal polymer: MCh (mg)	Plasticizer: propylene glycol (mg)	External polymer		Plasticizer		Dosage of active substance (mg)
			Alginate (mg)	Hyaluronate (mg)	Glycerol (mg)	Propylene glycol (mg)	
A1	600	50	500	—	—	25	200
A2	600	50	500	—	40	—	200
H1	600	50	—	500	—	25	200
H2	600	50	—	500	40	—	200
A3	600	50	500	—	—	25	100
A4	600	50	500	—	40	—	100
H3	600	50	—	500	—	25	100
H4	600	50	—	500	40	—	100

The crosslinking agent was  $\text{CaCl}_2$  (1.11 mg in the internal polymer and 55.5  $\mu\text{g}$  in the external polymer).

suitable mass (ca. 100 mg) and shape (cone) after drying in an Eppendorf tube with a capacity of 1.5 mL. The final scaffolds were characterized by a suitable plasticity and mechanical resistance and the ability to absorb water.

## Methods

**Size Determination and Morphological Characterization.** The structure of the preparations was studied with scanning electron microscopy (SEM). The measurements were performed under high vacuum with an FEI Nova NanoSEM 450. An accelerating voltage of 2 kV was used, and the distance of the electron gun from the sample was 5 mm. Fast-drying silver paint (Ted Pella, Inc.) was used to fix the samples onto the specimen mount.

**Mechanical Studies.** The mechanical properties of the chosen formulations were examined previously<sup>19</sup> by texture profile analysis (TPA) with a Stable Micro Systems Texture Analyzer TA-TX2. The analytical probe was compressed twice in each sampler with a trigger force of 5 g at a rate of 5.00 mm/s. A delay period of 5 s was allowed between the end of the first compression and the beginning of the second compression. All tests were performed at ambient temperature. The parameters that could be derived from TPA were as follows: *hardness*, that is, the force required to attain a given deformation; *springiness* (originally called *elasticity*), this being the ratio of the time required to achieve maximum structural deformation in the second compression cycle, where successive compressions were separated by a defined recovery period; and *cohesiveness*, this being the ratio of the area under the force–time curve produced on the first compression cycle, where successive compressions were separated by a defined recovery period.

**Mucoadhesiveness Studies.** The mucoadhesiveness of the polymeric membranes were evaluated by the modification of existing test methods through the introduction of silicone discs and a 10% solution of mucin.<sup>35</sup> The use of silicone discs allowed various tensometric measurements, which were reliable and reproducible, to be made. The advantage of silicone material, because of its mechanical strength and chemical and physical resistance, allowed us to use a new test method with a TA.WT2 texture analyzer (Stable Micro Systems, Surrey, United Kingdom). In this study, we examined various types of polymeric

matrices and their crosslinking and compared the concentrations of active substance within them to the pure dosage form.

**Swelling Characterization of the Inner Part.** Chitosan cones (ca. 100 mg) were introduced in a glass bottle containing 100 mL of phosphate buffer (pH 7.35) and incubated in a thermostated water bath under standard conditions or in the mobile state at a frequency of 100 movements per minute and an amplitude of 8 at  $37 \pm 0.5^\circ\text{C}$  with a mechanical water-bath shaker type 357 ELPIN<sub>sc</sub>+ (Conbest, Kraków, Poland). The weights of the cones were measured at appropriate time intervals with respect to their initial dry weights. The swollen cones were periodically removed and blotted with filter paper, and their changes in weight were measured during swelling until equilibrium was attained. Finally, the weights of the swollen cones were recorded (on an electronic balance) after a period of 24 h. The swelling index of the cones at various time periods was then calculated with the following formula<sup>36</sup>:

$$\text{Swelling index} = (w_t - w_0) / w_0 \times 100\% \quad (1)$$

where  $w_0$  is the initial weight of the dry cone and  $w_t$  is the weight of the swollen cone at equilibrium swelling in the medium.

**Fourier Transform Infrared (FTIR) Spectrophotometric Measurements.** Polymeric thin films were prepared for the FTIR studies. The formed solution of the coagulation of Alg or Hial with the drug ( $\text{Lid}_{\text{HCl}}$ ) and plasticizer (propylene glycol) was put onto a Teflon plate and left to dry at room temperature ( $25 \pm 2^\circ\text{C}$ ). Then, the polymer film was removed and used in the FTIR measurements on a PerkinElmer FTIR System Spectrum BX spectrophotometer. A total of 10 scans were accumulated. The spectral resolution was  $4 \text{ cm}^{-1}$ . The FTIR spectra were obtained over the wavelength range  $4000\text{--}400 \text{ cm}^{-1}$ . For comparison, polymer membranes with Alg and Hial in the absence of  $\text{Lid}_{\text{HCl}}$  were prepared as well. Separately, the IR spectra of  $\text{Lid}_{\text{HCl}}$  were taken with KBr pellets.

**Cytotoxicity Testing by 3-(4,5-dimethylthiazol-2-yl)-2,5-diphenyltetrazolium bromide (MTT) Assay.** The potential cytotoxic effects of the drug-delivery formulations were evaluated in a classic MTT reduction assay with L929 mouse

fibroblasts used as target cells. The MTT assay is a quantitative colorimetric method used to determine cell death with the activity of mitochondrial succinic dehydrogenase, which converts the water-soluble salt MTT into insoluble purple formazan; this is further dissolved in a dimethyl sulfoxide solution. The intensiveness of the color is directly proportional to the amount of the reaction product formed and, indirectly, to the number of live cells after the assay.<sup>37</sup> L929 fibroblasts obtained from American Type Culture Collection (ATCC; Rockville, MD) were selected because of their reproducible growth rates and biological responses, which have been well established by many authors to be suitable for cytotoxic assays of dental materials.<sup>38</sup> Mouse fibroblasts were grown in an RPMI-1640 medium supplemented with 10% fetal bovine serum, 2 mM L-glutamine, and antibiotics, penicillin (100 U/mL) and streptomycin (100 µg/mL), under standard conditions ( $37 \pm 0.5^\circ\text{C}$ ) in an incubator with a humidified atmosphere containing 5%  $\text{CO}_2$ . The cell cultures were supplemented with fresh medium two or three times per week to maintain them in the log phase. Before cytotoxicity determination, the cells were kept in antibiotic-free medium to prevent synergistic interaction between the antibiotics and the active substances dispersed inside polymeric preparations. To analyze the cytotoxicity of the obtained formulations,  $2 \times 10^5$  L929 cells/well were seeded into 96-well plates; polymeric formulations were added to the wells in triplicate and incubated under standard conditions for 24, 48, and 72 h. Exposure of the cells was stopped by the removal of the formulations, and the cell viability was immediately recorded by quantification of the reduction of MTT to formazan. Briefly, the MTT solution was added to each well (10 µL/mL). After 4 h of incubation ( $37 \pm 0.5^\circ\text{C}$ , 5%  $\text{CO}_2$ ), the supernatant was removed, and the MTT formazan stored intracellularly was solubilized in 200 µL of dissolving solution for 8 h at room temperature. The absorbance intensity in each well was measured at a wavelength of 570 nm with a plate-reading Victor<sub>2</sub> spectrophotometer (Wallac, Turku, Finland). Eight different formulations (Table I) were tested, as presented later in Figure 6.

**Determination of the  $\text{Lid}_{\text{HCl}}$  *In Vitro* Release.** The study was performed in a European Pharmacopeia (Ph. Eur.) flowthrough apparatus for release (Sotax USP 4 CE 1 Smart, Switzerland). Each of the formulations was placed in a cell for implants; the cell was closed with the prepared formulation and three sieves. The experiment was conducted in a closed system at  $37 \pm 0.5^\circ\text{C}$ ; the medium [100 mL of phosphate-buffered dissolution medium (phosphate-buffered saline) at pH 7.35] was circulated and was not replaced with a fresh solution. The parameters of the experiment were adjusted to the conditions measured in periodontium with laser Doppler flowmetry.<sup>39,40</sup> The absorbance and accumulated drug concentration was assayed online at a  $\lambda$  of 262 nm with a Thermo Scientific Evolution 300 ultraviolet–visible spectrophotometer with the computer program VisionPro (Spectro-Lab Warsaw, Poland) in a flow quartz cuvette (Starna Scientific, Ltd., type 71/Q/10, Material Spectrosil, path length = 10 mm). The  $\text{Lid}_{\text{HCl}}$  concentration was calculated with the following regression equation:

$$y = (0.6677 \pm 0.0035)x$$

where  $y$  is the absorbance and  $x$  is the concentration of  $\text{Lid}_{\text{HCl}}$

in the tested samples (mg). The standard calibration curve in the dissolution medium was linear over the range 1–100 mg/mL [determination coefficient ( $R^2$ ) = 0.999]. The results are reported as an average of four determinations.

**Mechanism of Drug Release.** Drug release from the polymeric formulations followed different kinetic orders: zero-order kinetics, which describes systems where the drug-release rate is independent of the concentration [eq. (2)]; first-order kinetics, where the drug-release rate from the system is dependent on the concentration [eq. (3)]; and Higuchi model kinetics [see eq. (4)] as the cumulative percentage of drug release versus the square root of time.

**Zero-order model.** The drug release from the dosage form follows a steady-state release running at a constant rate:

$$M_t/M_\infty = kt \quad (2)$$

where  $M_t$  is the amount of the drug released at time  $t$ ,  $M_\infty$  is the total amount of released drug at infinite time or equilibrium, and  $k$  is the rate constant of drug release.

**First-order model.** The drug activity within the reservoir is assumed to decline exponentially, and the release rate is proportional to the residual activity:

$$M_t/M_\infty = 1 - \exp(-kt) \quad (3)$$

**Higuchi model.** The Higuchi model<sup>41</sup> describes the release of drugs from the formulation as the square root of a time-dependent process on the basis of Fickian diffusion:

$$M_t/M_\infty = k_H t^{1/2} \quad (4)$$

where  $M_t/M_\infty$  is the fractional release or percentage release of the drug at time  $t$  and  $k_H$  is the Higuchi constant.

To evaluate the mechanism of drug release from the polymeric formulations, the release data were analyzed with the well-known semiempirical equation<sup>42–44</sup>:

$$M_t/M_\infty = Kt^n \quad (5)$$

where  $K$  is a kinetic constant that is characteristic of the drug/polymer system and  $n$  is the release exponent, which indicates the type of drug-release mechanism. The values of  $n$  were estimated by the linear regression of  $\log(M_t/M_\infty)$  versus the log time. If  $n$  approaches 0.5, the release mechanism can be Fickian (case I). This specific case is also referred to as the Higuchi model. If  $n$  approaches 1, the release mechanism can be zero order, whereas when  $0.5 < n < 1$ , non-Fickian (anomalous) transport can be obtained.

The kinetics of the drug release for the presented formulations as described previously<sup>45</sup> could be depicted as the first-order equation with two exponential functions:

$$M_t/M_\infty = A_0 + A_1[1 - \exp(-k_1 t)] + A_2[1 - \exp(-k_2 t)] \quad (6)$$

where  $A_0$  is the percentage of substance not released from the surface and bonded with the polymeric formulation,  $A_1$  is the percentage of substance released during the first phase,  $A_2$  is the percentage of substance released during the second phase, and  $k_1$  and  $k_2$  are the rate constants for the first and second release phases.

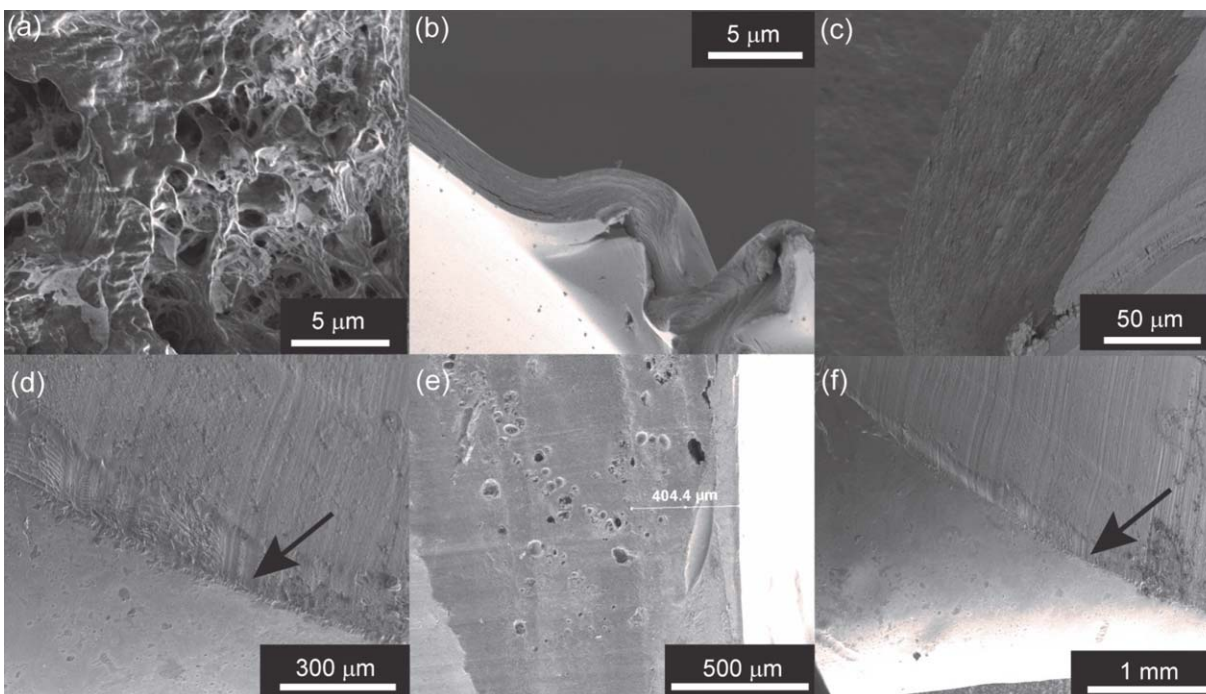


**Figure 1.** SEM images of the (a) cross-sectional morphology of MCCh, (b) surface and cross section of Hial with Lid<sub>HCl</sub>, (c) surface and cross section of Alg with Lid<sub>HCl</sub>, (d,f) cross section of a chitosan cone covered with a hyaluronate membrane, and (e) cross section of a chitosan cone covered with an alginate membrane. The arrows depict the outer part of the composite formulation. [Color figure can be viewed in the online issue, which is available at [wileyonlinelibrary.com](http://wileyonlinelibrary.com).]

**Statistical Analysis.** Statistical analysis was performed with the Microsoft Excel Analysis Tool Pak in Microsoft Office Excel 2010 and with Statistica 10. The experimental data had a normal distribution and were statistically assessed with the multi-factor analysis of variance method with a Duncan test  $\alpha$  of 0.05 embedded into the StatSoft STATISTICA 10 software package.

## RESULTS AND DISCUSSION

An appropriate process of matrix preparation allowed the uniform dispersal of the active substance to be obtained. Lid<sub>HCl</sub> was incorporated into the hydrogel by *in situ* loading.<sup>46</sup> The appropriate selection of excipients, that is, the plasticizer and the crosslinking agent, was another essential aspect of this study. It was important to release the active substance from a nonhomogeneous gel structure that was not fully crosslinked. The transformation of a homogeneous hydrogel of Alg into a solid homogeneous calcium alginate form by fully crosslinking calcium ions resulted in a slower diffusion of lidocaine. Hydrogel formation was favored because calcium alginate gels have a significantly higher affinity than Alg gels toward Ca<sup>2+</sup> ions. However, the addition of Ca<sup>2+</sup> was important for the formation of partial crosslinking of the alginate/hyaluronate, which was needed to maintain the viscosity of the nonhomogeneous gel described previously by the partial modification of the polymer structure through the partial exchange of Na<sup>+</sup> for Ca<sup>2+</sup>; this increased the mass transfer of lidocaine to the target. This effect was due to Ca<sup>2+</sup> salts being much less soluble than Na<sup>+</sup> salts; this reduced the affinity of lidocaine to the hydrogel. The diffusion of the drug from the matrix decreased as the concentration

of CaCl<sub>2</sub> solution increased because of the greater crosslinking of the hydrogel.<sup>47</sup>

## SEM

The formulations were prepared so that the active substance could be released from the external membrane while the inner core served as a scaffold. The SEM images of Alg/MCCh and Hial/MCCh formulation are shown in Figure 1. We observed that the surface of the external part of both matrices was relatively smooth with no aggregates of lidocaine. The membrane was monophasic [Figure 1(a–c)]. A cross section of the chitosan part showed irregularly placed pores with a size of 1–5  $\mu\text{m}$ . Thanks to the porous structure of the inner part of the formulation, the material constituted an appropriate space for cell migration. A scanning electron microscope was used to evaluate the structure of the materials obtained with their surface breakdown, microcracking, and voids taken into account.

Figure 1(d–f) presents the composite formulation with an emphasis on the adherence of the alginate [Figure 1(e)] and hyaluronate membranes [Figure 1(d,f)] to the chitosan cone.

## Mechanical Studies

A previous mechanical study incorporating TPA<sup>19</sup> revealed that although a hyaluronate membrane had no influence on the hardness of the chitosan polymer scaffold, Alg increased the strength. Similarly, the process of coating with hyaluronate was found to have no significant effect on the springiness (elasticity) or cohesiveness. Formulations with active substances showed lower springiness and cohesiveness values; these influenced the structure (Table II). An important finding by the previous study

**Table II.** Mechanical Characterization of the Simple and Composite Polymeric Formulations

Internal polymer	External polymer	Hardness (N)	Springiness (—)	Cohesiveness (—)
MCCh	—	78.0 ± 1.44	0.470 ± 0.022	0.562 ± 0.024
MCCh	Alg + Lid <sub>HCl</sub>	172.0 ± 1.48	0.507 ± 0.041	0.508 ± 0.087
MCCh	Hial + Lid <sub>HCl</sub>	19.5 ± 0.58	0.525 ± 0.081	0.501 ± 0.045

was that the material was deformed rather than destroyed or crushed during hardness testing; this was a perfect example of its elastic properties and highlighted its importance within the application process.

### Mucoadhesiveness Studies

In a previous experiment,<sup>35</sup> gels were not applied to chitosan cones but to previously prepared silicone discs. Various types of polymeric matrixes and crosslinking were examined, and the presence as the active substance was compared to that of the pure dosage form. Lid<sub>HCl</sub> was used as a model active substance because of its use in dentistry and clinical safety. We found that the alginate membranes showed high mucoadhesion, whereas the hyaluronic membrane Hial(Na<sup>+</sup>) without the crosslinking agent showed lower mucoadhesion. The addition of crosslinking agent increased the mucoadhesion, whereas the addition of the active substance decreased it. The lowest adhesion was observed for hyaluronate membranes with lidocaine Hial + Lid<sub>HCl</sub>(Ca<sup>++</sup>), as shown in Table III. In the SEM section, Figure 1(d–f) presents the composite formulation with an emphasis on the adherence of the alginate [Figure 1(e)] and hyaluronate membranes [Figure 1(d,f)] to the chitosan cone.

### Swelling Studies

The swelling process played an important role in the experiment. The absorption of liquid increased the volume and allowed the gel to fit to the site of application.

The polymers that we used were characterized by their ability to absorb large quantities of liquid. The system was designed so that the liquid-absorbing tissue formed a moist environment in the wound; this promoted the conditions required for the physiological healing of the alveolar process. The analysis was performed under two conditions: stable and in motion. The swelling kinetics and time-dependent swelling behaviors in a pH 7.35 buffer solution at 37 ± 0.5°C are plotted in Figure 2 as averages of six trials. The swelling data, which depended on factors by grouping, were analyzed with multivariate analysis of

**Table III.** Mucoadhesion of the Polymeric Materials Forming the Outer Layer of the Complex Systems

External polymer	Mucoadhesive work (J)
Alg(Na <sup>+</sup> )	1.62 ± 0.06
Alg(Ca <sup>++</sup> )	1.69 ± 0.03
(Alg + Lid <sub>HCl</sub> )(Ca <sup>++</sup> )	1.22 ± 0.02
Hial(Na <sup>+</sup> )	0.60 ± 0.04
Hial(Ca <sup>++</sup> )	0.68 ± 0.02
(Hial + Lid <sub>HCl</sub> )(Ca <sup>++</sup> )	0.40 ± 0.01

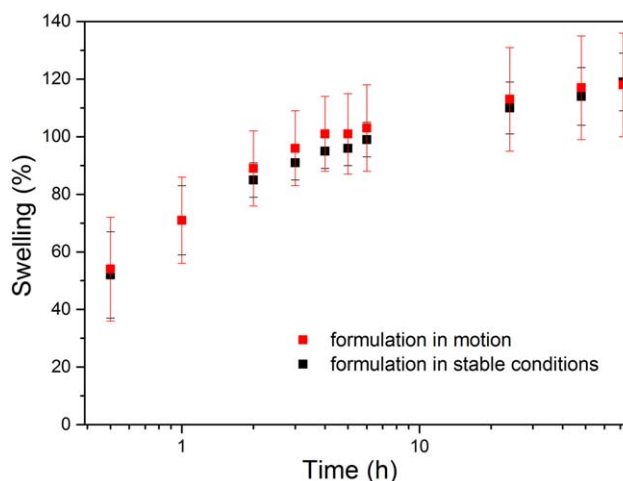
variance in repeated measurements (in each case, one of the factors was the time of the measurement) and *post hoc* analysis was performed with Tukey's test.

The analysis of the swelling process indicated that the site of application could be protected by the ability of the material to absorb water, as initially assumed.

The experiment was carried out under two different conditions: static conditions and in motion, and there was no significant difference ( $p = 0.3709$ ) in the results of the swelling, regardless of whether the formulation was shaken (119%) or not (118%). The interaction between the time of measurement and the conditions of the study was not significant ( $p = 0.4040$ ); this meant that the shaking of the formulation did not significantly affect the swelling process. The main aim of this study according to conditions was to confirm the resistance of the material to destruction. This material was capable of absorbing amounts of water greater than 100 wt %.

### FTIR Spectroscopy Analysis

FTIR studies of the Alg and Hial films with and without the active substance (Lid<sub>HCl</sub>) were performed to characterize the chemical structure of the outer part of the formulations and the correlation between the active substance interactions with the matrix. The FTIR spectra of Hial and Alg from thin films with and without Lid<sub>HCl</sub> are shown in Figures 3 and 4. An additional spectral IR line of pure Lid<sub>HCl</sub> is shown. This analysis was important in the aspect of explaining the kinetics of release of lidocaine from different membranes.

**Figure 2.** Swelling ability of the MCCh formulations in a moving medium and in a stable environment at 37 ± 0.5°C. [Color figure can be viewed in the online issue, which is available at wileyonlinelibrary.com.]

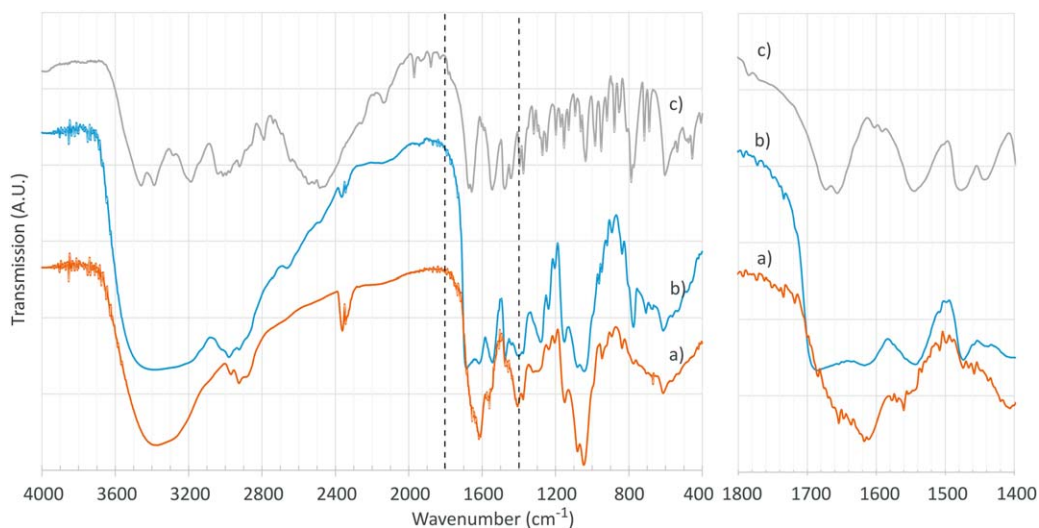


**Figure 3.** FTIR spectra obtained from the thin polymer films of Hial with and without Lid<sub>HCl</sub>: (a) Hial, (b) Hial + Lid<sub>HCl</sub>, and (c) Lid<sub>HCl</sub>. The comparative spectrum for Lid<sub>HCl</sub> was taken with KBr pellets. [Color figure can be viewed in the online issue, which is available at [wileyonlinelibrary.com](http://wileyonlinelibrary.com).]

In free Hial, the broad band visible from the high wave-number side of the spectrum ( $3376\text{ cm}^{-1}$ ) due to hydrogen-bond interaction was attributed to the O—H stretching vibrations. Moreover, the C—H stretching bands were identified as doublets at  $2966/2926\text{ cm}^{-1}$  [Figure 3(a)]. Hyaluronan is a copolymer composed of two repeating disaccharides: D-glucuronic acid and N-acetyl glucosamine. The spectrum of the Hial film [Figure 3(a)] exhibited several highly overlapping bands in the region of the carbonyl stretching vibrations ( $1800\text{--}1500\text{ cm}^{-1}$ ) derived from the vibrations of the acetamide ( $\text{CH}_3\text{CONH}_2$ ) and carbonyl groups ( $\text{C}=\text{O}$ ) present in the N-acetyl glucosamine and D-glucuronic acid units, respectively.<sup>48</sup> The highest peak occurring in this region ( $1618\text{--}1616\text{ cm}^{-1}$ ) was assigned to the antisymmetrical stretching vibrations in the carbonyl group of the carboxylate ( $\text{COO}^-$ ). Overlapping with this band were the amide I and amide II bands of the acetamide group. On the left side of the  $\text{COO}^-$  peak as a discrete shoulder ( $1636, 1647, \text{ and } 1654\text{ cm}^{-1}$ )

appeared the amide I band, and on the right side, appearing as a larger shoulder ( $1576, 1570, \text{ and } 1560\text{ cm}^{-1}$ ), was the amide II band.

The Hial–Lid<sub>HCl</sub> spectrum [Figure 3(b)] showed all of the characteristic bands of the polymer; however, the intensity of the band at approximately  $1618\text{ cm}^{-1}$ , characteristic of the carbonyl group, decreased significantly in the presence of Lid<sub>HCl</sub>. Moreover, a peak deformation at  $1700\text{--}1600\text{ cm}^{-1}$  and a new band at  $1685\text{ cm}^{-1}$  were detected for the Hial–Lid<sub>HCl</sub> layer. The shape of the spectrum and the results of the determinations of the pharmaceutical availability of Lid<sub>HCl</sub> from the polymer matrix in the HialNa outer layer indicated a weak interaction between the drug substance and the polymer.

The FTIR spectrum of the Alg films [Figure 4(a)] showed a broad band at about  $3429\text{ cm}^{-1}$ ; this corresponded to O—H stretching vibrations. In addition, a sharp peak was also visible

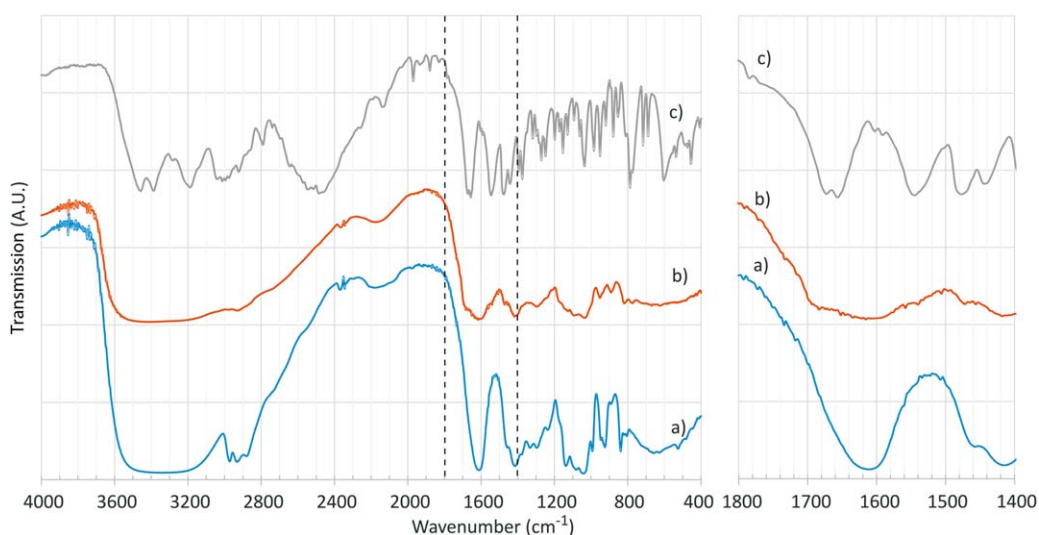


**Figure 4.** FTIR spectra obtained from the thin polymer films of Alg with and without Lid<sub>HCl</sub>: (a) Alg, (b) Alg + Lid<sub>HCl</sub>, and (c) Lid<sub>HCl</sub>. The comparative spectrum of Lid<sub>HCl</sub> was taken with KBr pellets. [Color figure can be viewed in the online issue, which is available at [wileyonlinelibrary.com](http://wileyonlinelibrary.com).]

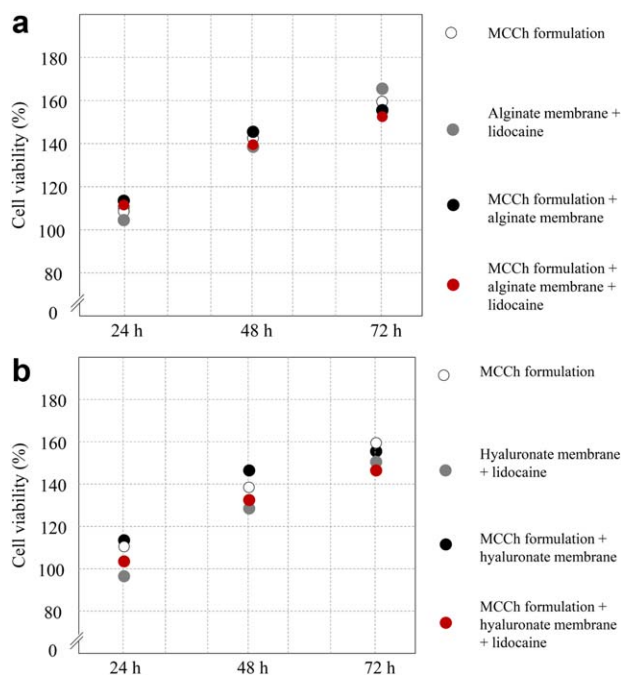


**Figure 5.** Effects of various polymeric formulations with (a) alginate and (b) hyaluronate on the viability of the L929 fibroblasts with 24, 48, and 72 h of incubation as measured with the MTT reduction assay. Each experiment was performed in triplicate with four technical repeats. The mean values for all of the experiments are presented. [Color figure can be viewed in the online issue, which is available at [wileyonlinelibrary.com](http://wileyonlinelibrary.com).]

at 2970 and 2932  $\text{cm}^{-1}$  and was due to C–H stretching vibrations in the spectra. The asymmetric and symmetric stretching of the  $-\text{COO}$  group of alginate was observed at 1610 and 1416  $\text{cm}^{-1}$ , respectively.<sup>49</sup>

FTIR spectral analysis for the Alg–Lid<sub>HCl</sub> [Figure 4(b)] preparations showed a reduction in the intensity in all of the bands, especially at 2800–3000  $\text{cm}^{-1}$ . In the presence of Lid<sub>HCl</sub>, the spectra became poorly marked within this range; this was most likely a result of overlapping by the Lid<sub>HCl</sub> line. Similar to Hial–Lid<sub>HCl</sub>, a peak deformation at 1700–1600  $\text{cm}^{-1}$  and a new weak

band at 1688  $\text{cm}^{-1}$  were detected for the Alg–Lid<sub>HCl</sub> layer. Moreover, there were no additional bands characteristic of the new functional groups in addition to those typical of lidocaine and alginate. No additional covalent bonds were formed.

The shape of the spectrum and the results of determinations of pharmaceutical availability of Lid<sub>HCl</sub> from the polymer matrix in the AlgNa outer layer indicated a weak interaction between the drug substance and the polymer.

### Cell Viability

The evaluation of the toxicity of the materials was performed with MTT testing by the direct contact of L929 cells with the material tested. The MTT assay is a widely used and accepted method for the assessment of cell viability.<sup>50</sup> Although chitosan is recognized as a nontoxic polymer, some studies have denied that fact. In this study, we performed a cytotoxicity evaluation to clarify the nontoxic nature of the formulations with all of the components. The cell viability after incubation with the tested preparations was expressed as a percentage of cells able to reduce MTT in comparison with the untreated culture; this was considered 100% viability. After 48 and 72 h of incubation, the cells proliferated naturally and expanded in all cultures to a similar extent. No statistical differences between the samples tested were observed. On the basis of these data, we concluded that tested formulations did not affect the viability or natural proliferation of fibroblasts.

As shown in Figure 5, neither MCCh cones alone or covered with hyaluronate or alginate nor the formulations with Lid<sub>HCl</sub> reduced the viability of the L929 fibroblasts.

### In Vitro Release of Lid<sub>HCl</sub>

The purpose of this part of the study was to achieve a controlled prolonged drug release with an initial rapid phase caused by a high-concentration gradient of the drug between the matrix surface and the medium (phosphate-buffered saline). The release of lidocaine was determined for eight kinds of formulations containing different polymers, different plasticizers, and two concentrations of the active substance. The kinetics of drug release are illustrated in Figures 6 and 7. On the basis of

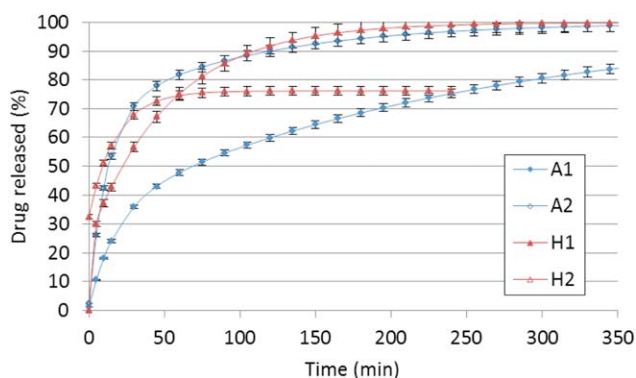


**Figure 6.** Release profiles of Lid<sub>HCl</sub> (200 mg) from different formulations [AlgGP–MCCh (A1), AlgG–MCCh (A2), HialGP–MCCh (H1), and HialG–MCCh (H2)] into a phosphate buffer (pH 7.35) at  $37 \pm 0.5^\circ\text{C}$ . The means and standard deviations ( $n = 4$ ) are presented. [Color figure can be viewed in the online issue, which is available at [wileyonlinelibrary.com](http://wileyonlinelibrary.com).]

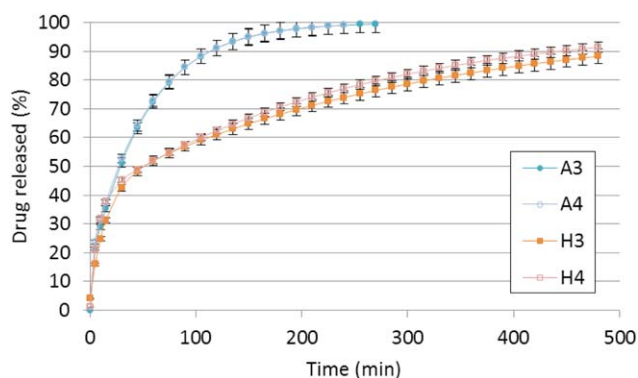


**Figure 7.** Release profiles of Lid<sub>HCl</sub> (100 mg) from different formulations [AlgGP–MCCh (A3), AlgG–MCCh (A4), HialGP–MCCh (H3), and HialG–MCCh (H4)] into a phosphate buffer (pH 7.35) at  $37 \pm 0.5^\circ\text{C}$ . The means and standard deviations ( $n = 4$ ) are presented. [Color figure can be viewed in the online issue, which is available at [wileyonlinelibrary.com](http://wileyonlinelibrary.com).]



**Table IV.** Parameters and  $R^2$  Values of Different Models

Formulation	Kinetic models									
	Zero order [eq. (2)]		First order [eq. (3)]		Higuchi [eq. (4)]		Korsmeyer-Peppas [eq. (5)]			
	$k$ (%/min)	$R^2$	$k$ ( $\text{min}^{-1}$ )	$R^2$	$k_H$ (% $\text{min}^{-0.5}$ )	$R^2$	$K$ ( $\text{min}^{-n}$ )	$n$	$R^2$	
A1	$0.3958 \pm 0.0283$	0.8744	$0.0198 \pm 0.0017$	<b>0.9775</b>	$5.266 \pm 0.098$	<b>0.9722</b>	$9.14 \pm 0.70$	$0.389 \pm 0.015$	<b>0.9880</b>	
A2	$1.0018 \pm 0.1351$	0.7819	$0.0631 \pm 0.0051$	<b>0.9779</b>	$9.715 \pm 0.497$	<b>0.9018</b>	$23.39 \pm 2.87$	$0.294 \pm 0.029$	<b>0.9410</b>	
H1	$1.3152 \pm 0.1787$	<b>0.9575</b>	$0.0606 \pm 0.0103$	<b>0.9403</b>	$9.971 \pm 0.307$	<b>0.9946</b>	$15.61 \pm 0.66$	$0.381 \pm 0.011$	<b>0.9960</b>	
H2	$0.7336 \pm 0.1146$	0.6641	$0.1216 \pm 0.0117$	<b>0.9140</b>	$8.110 \pm 0.626$	0.8197	$37.53 \pm 2.52$	$0.156 \pm 0.016$	<b>0.9164</b>	
A3	$0.8201 \pm 0.0673$	<b>0.9271</b>	$0.0255 \pm 0.0029$	<b>0.9796</b>	$8.626 \pm 0.121$	<b>0.9908</b>	$11.61 \pm 0.68$	$0.434 \pm 0.013$	<b>0.9946</b>	
A4	$0.6329 \pm 0.0541$	0.8722	$0.0269 \pm 0.0022$	<b>0.9824</b>	$7.920 \pm 0.220$	<b>0.9471</b>	$16.42 \pm 1.62$	$0.349 \pm 0.021$	<b>0.9708</b>	
H3	$0.3517 \pm 0.0282$	0.8314	$0.0248 \pm 0.0028$	<b>0.9494</b>	$5.155 \pm 0.155$	<b>0.9514</b>	$14.86 \pm 0.85$	$0.294 \pm 0.011$	<b>0.9820</b>	
H4	$0.3184 \pm 0.0233$	0.8673	$0.0221 \pm 0.0029$	<b>0.9077</b>	$5.124 \pm 0.145$	<b>0.9724</b>	$16.80 \pm 0.40$	$0.277 \pm 0.004$	<b>0.9958</b>	

The means and standard deviations are presented. Number of bold  $R^2 > 0.9$ .

**Table V.** Constant Values of the Kinetic Equation [Eq. (6)] Describing  $\text{Lid}_{\text{HCl}}$  Release from the Formulations

Formulation	First-order model with two exponential functions [eq. (6)]									
	$A_0$ (%)	$A_1$ (%)	$k_1$ ( $\text{min}^{-1}$ )	$t_{1\ 0.5}$ (min)	$A_2$ (%)	$k_2 \times 10^{-3}$ ( $\text{min}^{-1}$ )	$t_{2\ 0.5}$ (min)	$t_{2\ 0.9}$ (min)	$R^2$	
A1	1.1	$34.0 \pm 1.4$	$0.0554 \pm 0.0047$	$12.51 \pm 0.98$	$64.9 \pm 1.3$	$4.00 \pm 0.14$	$173.3 \pm 5.9$	$576 \pm 20$	0.9984	
A2	2.3	$66.0 \pm 9.1$	$0.0828 \pm 0.0165$	$8.37 \pm 0.78$	$31.7 \pm 9.3$	$9.70 \pm 3.72$	$71.4 \pm 19.8$	$237 \pm 65$	0.9878	
H1	0.0	$24.4 \pm 1.7$	$0.6008 \pm 0.0250$	$1.15 \pm 0.05$	$75.5 \pm 1.3$	$18.50 \pm 0.60$	$37.5 \pm 1.2$	$124 \pm 3$	0.9981	
H2	32.5	$43.6 \pm 3.3$	$0.0553 \pm 0.0098$	$12.53 \pm 1.89$	$23.8 \pm 2.2$	$0.47 \pm 0.01$	$1474 \pm 30.7$	—	0.9979	
A3	0.0	$14.0 \pm 3.1$	$0.8048 \pm 0.0225$	$0.86 \pm 0.02$	$86.0 \pm 2.3$	$19.00 \pm 0.77$	$36.5 \pm 1.4$	$121 \pm 5$	0.9957	
A4	0.0	$17.2 \pm 0.9$	$0.5755 \pm 0.1916$	$1.20 \pm 0.30$	$82.8 \pm 0.7$	$18.64 \pm 0.23$	$37.2 \pm 0.5$	$124 \pm 2$	0.9995	
H3	4.1	$37.9 \pm 3.5$	$0.0684 \pm 0.0140$	$10.13 \pm 1.72$	$58.0 \pm 2.9$	$3.34 \pm 0.32$	$207.5 \pm 18.1$	$689 \pm 60$	0.9793	
H4	1.1	$37.4 \pm 2.1$	$0.1400 \pm 0.0173$	$4.95 \pm 0.54$	$61.4 \pm 1.3$	$4.11 \pm 0.15$	$168.6 \pm 5.9$	$560 \pm 20$	0.9904	

The means and standard deviations are presented.  $t_{1\ 0.5}$  and  $t_{2\ 0.5}$ , the times at which the first and second steps reach 50% drug release, respectively;  $t_{2\ 0.9}$ , the time at which the second step reaches 90% drug release.

**Table VI.** Correlation between the Release Profiles for All Pairs of Lid<sub>HCl</sub> Formulations Given as  $R^2$  Values. Number of bold  $R^2 > 0.9$ 

Formulation	A1	A2	H1	H2	A3	A4	H3	H4
A1	1.0000							
A2	0.9303	1.0000						
H1	0.9448	0.9873	1.0000					
H2	0.8445	0.9791	0.9515	1.0000				
A3	0.9503	0.9814	<b>0.9980</b>	0.9433	1.0000			
A4	0.9501	0.9833	<b>0.9989</b>	0.9452	<b>0.9999</b>	1.0000		
H3	<b>0.9983</b>	0.9441	0.9509	0.8650	0.9537	0.9542	1.0000	
H4	<b>0.9941</b>	0.9364	0.9432	0.8495	0.9423	0.9439	<b>0.9967</b>	1.0000

the results, we noticed that the addition of excipients allowed a drug carrier with a varying half-life to be obtained. Depending on the type of plasticizer, the release of lidocaine from the formulations was obtained at different rates.

The initial rate of release of Lid<sub>HCl</sub> (200 mg) from the A2 formulation (Figure 6) was faster than that of formulations H1 (Figure 6) and A3 and A4 (Figure 7), but after 50 min, the release process slowed. The amount of lidocaine released from formulations A1 (Figure 6) and H3 and H4 (Figure 7) after 450 min was 90% of the total dosage. Formulations H1, A2 (Figure 6), and A3 and A4 (Figure 7) required a shorter period of time: approximately 120 min to release 90% of the total dosage. However, the release profile of formulation H2 (Figure 6) differed from the others, as the amount of released Lid<sub>HCl</sub> did not reach 90% by the end of the experiment: the maximum amount of the substance released was 76% and was reached after 240 min. This may have been caused by the different thicknesses of the hydrogel membrane, which affected the time of release of lidocaine.

The values of the measured parameters and the  $R^2$  values of the different kinetic equations are summarized in Table IV. It was not possible to obtain a good correlation by interpretation of the kinetics data for Lid<sub>HCl</sub> release as zero order [eq. (2)], as shown by the results of the correlation coefficients in Table IV, where all of the  $R^2$  values were below 0.90, except for those of A3 ( $R^2 = 0.9271$ ) and H1 ( $R^2 = 0.9575$ ).

In this study, all *in vitro* release profiles of Lid<sub>HCl</sub> from the obtained systems, except H2 ( $R^2 = 0.8197$ ), were well explained by the first-order model [eq. (3)], as the plots showed a high linearity, and  $R^2$  ranged from 0.9077 to 0.9824, and by the Higuchi model [eq. (4);  $R^2 = 0.9018$ –0.9946]. Moreover, the obtained results were plotted into the Korsmeyer–Peppas equation [eq. (5)] to determine the diffusion mechanism.

Korsmeyer and coworkers<sup>42–44</sup> derived a simple relationship that described the mechanism of drug release from a polymeric system. To determine the mechanism of Lid<sub>HCl</sub> release, first, 60% drug-release data were fitted into the Korsmeyer–Peppas model [eq. (5)]. The slopes and intercepts obtained from  $\log M_t/M_\infty$  versus  $\log$  time linear plots were used to calculate the values of  $n$  and  $k$  (see Table IV).

The release process of Lid<sub>HCl</sub> from most formulations, except the A2 ( $R^2 = 0.9410$ ) and H2 ( $R^2 = 0.9164$ ) formulations, were better described by the Korsmeyer–Peppas equation [eq. (5)]

with an  $R^2$  of 0.9708–0.9960. For all of formulations, the  $n$  values ranged from 0.156 to 0.434 (Table IV). This showed that for all of the formulations, the release mechanism was the Fickian (case I) release mechanism.<sup>42–44</sup>

Profiles of Lid<sub>HCl</sub> release (Figures 6 and 7) revealed that the drug release was a two-stage process with an initial faster effect and a slower second stage.<sup>45,51,52</sup> In the first phase, this process was a function of the change in the drug concentration in the surface layer, of which the total release of particles was more easily accessible. The second phase corresponded to the effective delayed release of the drug substance from the deeper layers of the polymer formulations. We assumed that in this phase, there was diffusion of the drug substances from the deeper layers of the formulation.

According to the release profiles, which indicated a two-phase process, the formulations had to be described by a first-order model with two exponential functions [eq. (6)]. The parameters of the composite kinetic equation are summarized in Table V; these demonstrate that eq. (6) was suitable for describing the release of Lid<sub>HCl</sub>.

The  $k$  values in eq. (6) may have played the role of kinetic constants; therefore, they may be useful for the comparison of the drug-release kinetics from various systems. The higher the  $k_1$  value is compared to that of  $k_2$  indicates that the rate of release is greater than that of diffusion.<sup>52</sup> In the majority of the experiments, in the second phase, the formulations showed a steady-state diffusion-controlled release.

The analysis of the data from Figures 6 and 7 and Table V indicated that the amount of Lid<sub>HCl</sub> released from the formulations was dependent on their properties and components. The formulations showed optimal release parameters, except the H2 formulation, fabricated from hyaluronate and glycerol as a plasticizer; this caused the lowest degree of release. The process of release clearly occurred in three phases (very fast to 5 min, rapid to 45 min, and much slower thereafter;  $t_{2,0.5} = 1474 \pm 30.7$  min).

The correlation, given as  $R^2$  values, between the release profiles for all pairs of Lid<sub>HCl</sub> formulations was calculated with Excel for data analysis (Table VI).

A correlation was observed between the level of Lid<sub>HCl</sub> release from the formulations and the composition of the system. By comparing the Lid<sub>HCl</sub> release profiles (Figures 6 and 7) for pairs of formulations, we observed high correlations ( $R^2 > 0.99$ ) for

the following pairs, which are given in bold in Table VI: A1 with H3 and A1 with H4, H1 with A3 and H1 with A4, and A3 with A4 and H3 with H4. For other pairs of formulations,  $R^2$  ranged from 0.93 to 0.99. Only for formulation pairs H2 with H3 and H2 with H4 was  $R^2$  less than 0.87.

The rate of release of Lid<sub>HCl</sub> (100 mg) from the hyaluronate layer did not depend on the type of plasticizer (H3 and H4). This rate was similar for the alginate layer A1, which contained a higher dose of Lid<sub>HCl</sub> (200 mg) and propylene glycol as the plasticizer. Similarly, the rate of release of Lid<sub>HCl</sub> (100 mg) from the alginate layers A3 and A4 did not depend on the type of plasticizer and was similar to that of the hyaluronate layer (H1), which contained a larger dose of Lid<sub>HCl</sub> (200 mg) and propylene glycol as the plasticizer.

For lower concentrations of Lid<sub>HCl</sub> (100 mg), the active substance was released more readily from the alginate than from the hyaluronate part, and the amount of Lid<sub>HCl</sub> released did not depend on the type of plasticizer. For higher concentrations of Lid<sub>HCl</sub> (200 mg), the rate of drug release was related to the type of plasticizer. Although the addition of propylene glycol to the alginate layer slowed down the release of Lid<sub>HCl</sub>, the opposite was true when it was added to the hyaluronate layer.

On the basis of the results obtained, we concluded that the rate of release of Lid<sub>HCl</sub> from the formulation was a result of the physical properties of the raw material (hydrogel). No chemical interaction was observed between the active substances, that is, the polymer and plasticizer. Differences in the rate of release of the biologically active substance may have resulted from the different densities of the hydrogels; this directly affected the coefficient of diffusion. It is known that with an increase in the density, the diffusion coefficient decreases; this slowed down the release of Lid<sub>HCl</sub> in hydrogels based on hyaluronan.

## CONCLUSIONS

The preliminary data strongly suggests that the formulations obtained are likely to be applied in practice. The hypothesis was confirmed; the results of the swelling studies indicate that the materials used formed a dressing that could protect the postextraction alveolus. Also, the formulations were topical drugs that released the active substance directly into the target. Drug release could be controlled through the appropriate selection of the polymer concentration and type of plasticizer. The results of this study confirm the importance of the selection of suitable polymers and excipients for controlled release.

The process of the release of Lid<sub>HCl</sub> from the studied formulations was of a two-phase nature. The first phase was characterized by rapid release, whereas the second phase was much slower; this is positive with regard to the drug-application assignment, that is, for giving a prolonged therapeutic effect. The faster effect indicated rapid water uptake by the polymeric formulation and the dissolution of the exposed Lid<sub>HCl</sub> particles at the surface of the formulation. The second process was slower, and it was caused by the swelling of the inner matrix layer and the absorption of acceptor fluid, together with the active substance.

The aim of the study was to determine a method for treating inflammation and administering anesthetic substances with available natural polymers and a simple manufacturing technique.

An MTT assay with L929 cells found the formulations to not be cytotoxic. The results suggest that the materials obtained have potential clinical applications.

Our results demonstrate the possible future use of a cone polymer system to treat such clinical complications as AO with clear future benefits for the health care system.

## ACKNOWLEDGMENTS

The study was financed through the statutory subject of the Medical University in Lodz (contract grant number 503/3-021-01/503-31-001). The SEM was financed by the EC7th FP under the Research Potential (Coordination and Support Actions FP 7-REGPOT-CT-2011-285949-NOBLESSE).

## REFERENCES

1. Noroozi, A.-R.; Philbert, R. F. *Oral Surg. Oral Med. Oral Pathol. Oral Radiol. Endod.* **2009**, *107*, 30.
2. Vezeau, P. J. *J. Oral Maxillofac. Surg.* **2000**, *58*, 531.
3. Birn, H. *Int. J. Oral Surg.* **1973**, *2*, 211.
4. Dash, M.; Chiellini, E.; Ottenbrite, R. M.; Chiellini, E. *Prog. Polym. Sci.* **2011**, *36*, 981.
5. Aranaz, I.; Mengibar, M.; Harris, R.; Paños, I.; Miralles, B.; Acosta, N.; Galed, G.; Heras, Á. *Curr. Chem. Biol.* **2009**, *3*, 203.
6. Bhattarai, N.; Gunn, J.; Zhang, M. *Adv. Drug Delivery Rev.* **2010**, *62*, 83.
7. Giri, T. K.; Thakur, A.; Alexander, A.; Badwaik, H.; Tripathi, D. K. *Acta Pharm. Sin. B* **2012**, *2*, 439.
8. Kim, C. H.; Park, H.-S.; Gin, Y. J.; Son, Y.; Lim, S.-H.; Choi, Y. J.; Park, K.-S.; Park, C. W. *Macromol. Res.* **2004**, *12*, 367.
9. Muzzarelli, R. A. A. *Carbohydr. Polym.* **2011**, *83*, 1433.
10. Shi, C.; Zhu, Y.; Ran, X.; Wang, M.; Su, Y.; Cheng, T. *J. Surg. Res.* **2006**, *133*, 185.
11. Ravi Kumar, M. N. V.; Muzzarelli, R. A. A.; Muzzarelli, C.; Sashiwa, H.; Domb, A. *J. Chem. Rev.* **2004**, *104*, 6017.
12. Säkkinen, M.; Marvola, J.; Kanerva, H.; Lindevall, K.; Lipponen, K. M.; Kekki, T.; Ahonen, A.; Marvola, M. *Eur. J. Pharm. Biopharm.* **2004**, *57*, 133.
13. Säkkinen, M.; Marvola, J.; Kanerva, H.; Lindevall, K.; Ahonen, A.; Marvola, M. *Int. J. Pharm.* **2006**, *307*, 285.
14. Struszczyk, H. *J. Appl. Polym. Sci.* **1987**, *33*, 177.
15. Hoekstra, A.; Struszczyk, H.; Kivekas, O. *Biomaterials* **1998**, *19*, 1467.
16. Pighinelli, L.; Kucharska, M.; Wiśniewska-Wrona, M.; Gruchała, B.; Brzoza-Malczewska, K. *Int. J. Mol. Sci.* **2012**, *13*, 7617.
17. Struszczyk, M. H. *Polimery* **2002**, *47*, 396.
18. Food and Drug Administration. ChitoClear® Shrimp-Derived Chitosan: Food Usage Conditions for General Recognition of Safety. GRAS Notice (GRN) No. 443. <http://www.fda.gov/ucm/groups/fdagov-public/@fdagov-foods-gen/>

- documents/document/ucm337459.pdf. Accessed on May 7, 2015.
19. Nowak, K. M.; Bodek, K. H. *Curr. Issues Pharm. Med. Sci.* **2013**, *26*, 254.
  20. Rehm, B. H. A. *Alginates: Biology and Applications; Microbiology Monographs 13; Springer-Verlag: Berlin, 2009.*
  21. Tønnesen, H. H.; Karlsen, J. *Drug Dev. Ind. Pharm.* **2002**, *28*, 621.
  22. Pawar, S. N.; Edgar, K. J. *Biomaterials* **2012**, *33*, 3279.
  23. Lee, K. Y.; Mooney, D. J. *Prog. Polym. Sci.* **2012**, *37*, 106.
  24. Teh, B. M.; Shen, Y.; Friedland, P. L.; Atlas, M. D.; Marano, R. J. *Expert Opin. Biol. Ther.* **2012**, *12*, 23.
  25. Solis, M. A.; Chen, Y.-H.; Wong, T. Y.; Bittencourt, V. Z.; Lin, Y.-C.; Huang, L. L. H. *Biochem. Res. Int.* **2012**, *2012*, 346972.
  26. Zhang, F.; He, C.; Cao, L.; Feng, W.; Wang, H.; Mo, X.; Wang, J. *Int. J. Biol. Macromol.* **2011**, *48*, 474.
  27. Jiang, D.; Liang, J.; Noble, P. W. *Annu. Rev. Cell Dev. Biol.* **2007**, *23*, 435.
  28. Nakamura, S.; Matsuura, N.; Tatsuya, I. *J. Endodont.* **2013**, *39*, 1369.
  29. Rirattanapong, P.; Vongsavan, K.; Kraivaphan, P.; Vongsavan, N.; Matthews, B. *Arch. Oral Biol.* **2013**, *58*, 1549.
  30. Shin, S.-C.; Cho, C.-W.; Yang, K.-H. *Int. J. Pharm.* **2004**, *287*, 73.
  31. Kinasiewicz, A.; Juszczak, M.; Mazurek, A. P.; Rowiński, W.; Pachecka, J.; Fiedor, P. *Acta Pol. Pharm. Drug Res.* **2000**, *57*, 455.
  32. Van der Weijden, F.; Dell'Acqua, F.; Slot, D. E. *J. Clin. Periodontol.* **2009**, *36*, 1048.
  33. Lekovic, V.; Kenney, E. B.; Weinlaender, M.; Han, T.; Klokkevold, P.; Nedic, M.; Orsini, M. *J. Periodontol.* **1997**, *68*, 563.
  34. Fickl, S.; Zuh, O.; Wachtel, H.; Bolz, W.; Huerzeler, M. *J. Clin. Periodontol.* **2008**, *35*, 356.
  35. Nowak, K. M.; Szterk, A.; Fiedor, P.; Bodek, K. H. *Acta Pol. Pharm. Drug Res.*, **2016**, *73*, 2 (to appear).
  36. Perioli, L.; Ambrogi, V.; Rubini, D.; Giovagnoli, S.; Ricci, M.; Blasi, P.; Rossi, C. *J. Controlled Release* **2004**, *95*, 521.
  37. Fischer, D.; Bieber, T.; Li, Y.; Elsaesser, H.; Kissel, T. *Pharm. Res.* **1999**, *16*, 1273.
  38. Thonemann, B.; Schmalz, G.; Hiller, K. A.; Schweikl, H. *Dent. Mater.* **2002**, *18*, 318.
  39. Retzepi, M.; Tonetti, M.; Donos, N. *J. Clin. Periodontol.* **2007**, *34*, 437.
  40. Kerdvongbundit, V.; Vongsavan, N.; Soo-Ampon, S.; Hasegawa, A. *Odontology* **2003**, *91*, 19.
  41. Higuchi, T. *J. Pharm. Sci.* **1963**, *52*, 1145.
  42. Korsmeyer, R. W.; Gurny, R.; Doelker, E.; Buri, P.; Peppas, N. A. *Int. J. Pharm.* **1983**, *15*, 25.
  43. Peppas, N. A. *Pharm. Acta Helv.* **1985**, *60*, 110.
  44. Nagy, J.; Folhoffer, A.; Horvath, A.; Csak, T.; Taba, G.; Szentmihályi, K.; Szalay, F.; Zelko, R. *Pharmazie* **2005**, *60*, 524.
  45. Bodek, K. H.; Nowak, K. M.; Kozakiewicz, M.; Bodek, A.; Michalska, M. *Int. J. Polym. Sci.*, **2015**, *2015*, <http://dx.doi.org/10.1155/2015/386251>.
  46. Lin, C.-C.; Metters, A. T. *Adv. Drug Delivery Rev.* **2006**, *58*, 1379.
  47. Rajinikanth, P. S.; Sankar, C.; Mishra, B. *Drug Delivery* **2003**, *10*, 21.
  48. Coimbra, P.; Alves, P.; Valente, T. A. M.; Santos, R.; Correia, I. J.; Ferreira, P. *Int. J. Biol. Macromol.* **2011**, *49*, 573.
  49. Devi, M. P.; Sekar, M.; Chamundeswari, M.; Moorthy, A.; Krithiga, G.; Murugan, N. S.; Sastry, T. P. *Bull. Mater. Sci.* **2012**, *35*, 1157.
  50. Mossmann, T. J. *Immunol. Methods* **1983**, *65*, 55.
  51. Park, S.-N.; Kim, J. K.; Suh, H. *Biomaterials* **2004**, *25*, 3689.
  52. Kubis, A. A.; Musiał, W.; Szcześniak, M. *Pharmazie* **2002**, *57*, 479.